5th International Conference on Durability of Concrete Structures
Jun 30–Jul 1, 2016
Shenzhen University, Shenzhen, Guangdong Province, P.R.China

Corrosion-Induced Concrete Cracking Model Considering Corrosion-Filled Paste

Jianfeng Dong, Yuxi Zhao, Yingyao Wu, and Weiliang Jin
Institute of Structural Engineering, Zhejiang University, Hangzhou 310058, Zhejiang, China

ABSTRACT

A T_{CP}–T_{CL} model is established to describe the relationship between the thickness of the corrosion-filled paste (CP) and that of the corrosion layer (CL). This model can describe the phenomenon that the corrosion filling in the concrete pores and accumulating at the steel/concrete interface occur synchronously. Based on the T_{CP}–T_{CL} model, a corrosion-induced concrete cracking model, which can quantitatively consider corrosion-filled paste at concrete/steel interface, is proposed. Combined with damage analysis in corrosion-induced cracking process of concrete cover, the model is developed to describe the quantity of steel corrosion required to crack the concrete surface.

1. INTRODUCTION

Steel corrosion is one of the most dominant causes of the deterioration of reinforced concrete structures (Bazant, 1979; Hartt, 2012). After steel depassivation, corrosion products are formed at the steel/concrete interface. Since the volume of the corrosion products is approximately two to six times the volume of the original steel (Cornell & Schwertmann, 1996; Marcotte & Hansson, 2007), it will produce pressure on the surrounding concrete. As the volume of the corrosion products increases, cracks initiate at the steel/concrete interface and propagate outward, eventually spreading to the surface of the concrete cover. These cracks provide a path for aggressive-agent rapid ingress to the reinforcement, which can accelerate the corrosion process according to Asami and Kikuchi (2003), Duffó, Morris, Raspini, and Saragovi (2004), Williamson and Clark (2000), and Ohtsu and Yosimura (1997). Therefore, investigation of the corrosion-induced cracking process is important for the prediction of the serviceability and durability of reinforced concrete structures.

To predict the corrosion-induced cracking time of the concrete cover quantitatively, the three-stage model proposed by Liu and Weyers (1998) has been widely accepted. In this model, the corrosion products causing concrete cracking are formed by three processes: (1) the corrosion products migrate to the pores at the steel/concrete interface before the pores are filled, and the corrosion products do not stress the surrounding concrete; (2) the corrosion products create the stress in the concrete cover after all of the pores at the steel/concrete interface are filled; and (3) the corrosion products crack the concrete cover and fill the corrosion-induced crack.

In the first stage, previous studies made by Chitty, Dillmann, Hostis, and Lombard (2005), Care, Nguyen, L'Hostis, and Berthaud (2008), Jaffer and Hansson (2009), Michel, Pease, Geiker, Stang, and Olesen (2011), and Zhao et al. (2012) determined an area of concrete around the steel penetrated by the corrosion products, i.e., a corrosion accommodating region (CAR) (Michel et al., 2011), or corrosion-filled paste (CP) (Wong, 2010). In this study, CP is used to indicate this region. The existence of CP has been verified for reinforced concrete members that had deteriorated in a natural environment (Asami & Kikuchi, 2003; Duffó et al., 2004; Michel et al., 2011), in artificial cyclic wet/dry tests by Jaffer and Hansson (2009) and Wong, Zhao, Karimi, Buenfeld, and Jin (2010) and during electrochemical corrosion (Care et al., 2008; Michel et al., 2011; Zhao et al., 2012). Although these studies have proven the existence of the CP, the actual value of CP, which can subsequently be used in the corrosion-induced concrete cracking model, has not yet been determined. The previous studies (Liu & Weyers, 1998; Lu, Jin, & Liu, 2011; Zhao & Jin, 2006) regarding the thickness of CP were all based on assumptions. Therefore, more research is needed to study the thickness of the CP and its variation with the growth of steel corrosion.

The second stage has been widely studied by Wong (2010), Zhao and Yu (2012), Li, Melchers, and Zheng (2006), Malumbela, Alexander, and Moyo (2011), Hansen and Saouma (1999), and Andrade, Alonso, and Molina (1993) in both experimental

and analytical research. Ignoring the pore-filling process, most of these models (Bazant, 1979; Chitty et al., 2005; Liu & Weyers, 1998; Zhao, Yu et al., 2011) focussed on the stressing and cracking process in the concrete cover induced by steel corrosion based on the theory of mechanics. However, according to the authors' recent work (Zhao, Wu, & Jin, 2013), the penetration of corrosion products into the porous zone of the concrete, i.e., the process of corrosion products filling pores, and the formation of a corrosion layer at the steel/concrete interface, i.e., the concrete cover stressing process, occur simultaneously with the initiation of steel corrosion. Hence, these phenomena should be included in the corrosion-induced concrete cracking model.

With respect to the third stage, previous studies made by Liu and Weyers (1998), Chitty et al. (2005), and Zhao, Yu et al. (2011) have assumed that corrosion products fill the corrosion-induced cracks. However, through experimental studies of different specimens, the corrosion products cannot fill the cracks before the initiation of concrete surface cracking according to the authors' results (Zhao et al., 2012, 2013). Therefore, there is no need to consider the Stage 3 in the corrosion-induced concrete surface cracking model.

The goal of the current study is to establish a corrosion-induced cracking model that can consider the corrosion product fill into paste at the steel/concrete interface and predict the concrete surface cracking more reasonably than the previous models. To achieve this goal, a relationship between the thickness of the CP and the thickness of the corrosion layer (CL) is initially modelled, then the conversion coefficient, α_n, is introduced to include the effect of corrosion filling in the paste. Combined with damage analysis in corrosion-induced cracking process of concrete cover, the model is developed to describe the quantity of steel corrosion required to crack the concrete surface.

2. CORROSION-INDUCED CRACKING MODEL CONSIDERING CP

2.1 Cracking process description

The cracking process of reinforced concrete caused by steel corrosion can be illustrated in Figure 1. After steel depassivation, some steel corrosion products accumulate in the steel/concrete interface to form the corrosion layer (CL). The thickness of the CL is T_{CL}. The remainder of the corrosion products fills the voids in the concrete around the steel to form the CP. The thickness of the CP is T_{CP}, as shown in Figure 1(b). With the development of the steel corrosion, T_{CP} increases as T_{CL} grows till the crack reaches the outer surface of concrete cover as Figure 1(c).

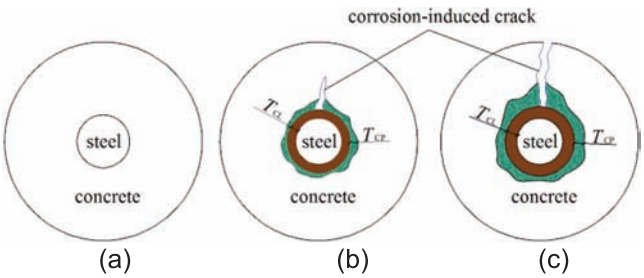

Figure 1. Corrosion-induced concrete cracking model considering corrosion-filled paste. (a) steel depassivation. (b) Corrosion-induced crack appears, CP and CL form simultaneously. (c) TCL and TCP increase gradually before crack reaches concrete outer surface.

2.2 T_{CP}–T_{CL} model

According to the authors' previous experimental results (Zhao, Ding, & Jin, 2014; Zhao et al., 2013), the average CP thickness increases as the CL thickness increases. However, when CL reaches a certain value, the average CP thickness has no obvious growth trend, as shown in Figure 2.

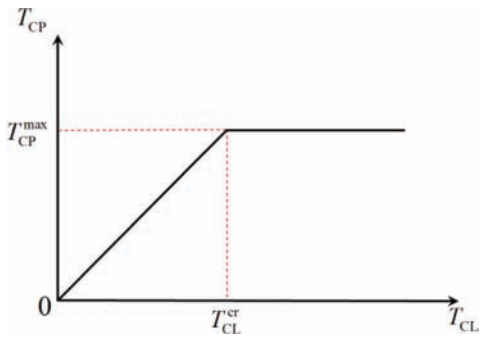

Figure 2. Relationship between T_{CP} and T_{CL} (Zhao et al., 2014, 2013).

Mathematically, this can be expressed as follows:

$$\begin{cases} T_{CP} = k_T \times T_{CL}, & T_{CL} < T_{CL}^{cr} \\ T_{CP} = T_{CP}^{max} = k_T \times T_{CL}^{cr}, & T_{CL} \geq T_{CL}^{cr} \end{cases} \quad (1)$$

where T_{CP}^{max} is the maximum T_{CP} achieved, T_{CL}^{cr} is the critical value of corrosion layer thickness corresponding to T_{CP}^{max}, and k_T is the ratio between T_{CP}^{max} and T_{CL}^{cr}.

To calculate CP in the concrete cracking model, CP is assumed to be an evenly distributed corrosion layer around the steel. The corrosion layer thickness of the distributed layer is defined as $T_{CL,\,pore}$, as shown in Figure 3. It needs to be pointed that uniformly distributed steel corrosion is an ideal state; in practical applications, most of the steel bars in concrete corrode non-uniformly.

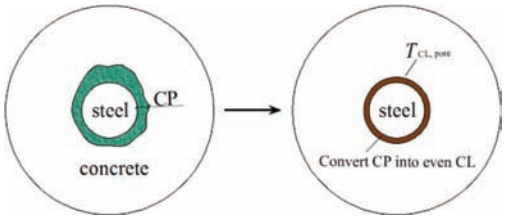

Figure 3. Conversion from the thickness of CP (T_{CP}) into the thickness of CL ($T_{CL,\,pore}$).

Assume that in the region of CP, the voids are filled completely with corrosion products, $T_{CL,pore}$ can be expressed as follows:

$$T_{CL,pore} = \frac{\phi \times \int_0^{2\pi} T_{CP} R\, d\theta}{2\pi R} \tag{2}$$

where ϕ is the porosity of the cement mortar around the steel bar in the concrete, R is the radius of the steel, and θ is the angle between the radius of the integral point and the starting point.

For uniform corrosion, CL is evenly distributed along the steel. The thickness of the CL is assumed equal to T_{CL}. Then, the average thickness of the fill area, T_{CP}, can be deduced from Eq. (1) as follows:

$$\begin{cases} \overline{T_{CP}} = k_T \times \overline{T_{CL}}, & \overline{T_{CL}} < T_{CL}^{cr} \\ \overline{T_{CP}} = T_{CP}^{max} = k_T \times T_{CL}^{cr}, & \overline{T_{CL}} \geq T_{CL}^{cr} \end{cases} \tag{3}$$

According to Eq. (2), $T_{CL,pore}$ can be expressed as follows:

$$T_{CL,pore} = \phi \times \overline{T_{CP}} \tag{4}$$

Combining Eq. (4) with Eq. (3), $T_{CL,pore}$ can be expressed as follows:

$$T_{CL,pore} = \begin{cases} \phi \times k_T \times \overline{T_{CL}}, & \overline{T_{CL}} < T_{CL}^{cr} \\ \phi \times T_{CL}^{max} = \phi \times k_T \times T_{CL}^{cr}, & \overline{T_{CL}} \geq T_{CL}^{cr} \end{cases} \tag{5}$$

It is well-known that the porosity of cement mortar depends on the quality of concrete. According to Eq. (5), $T_{CL,pore}$ also depends on the quality of the concrete. In practical applications, the value of k_T is determined from the relationship of T_{CP}–T_{CL}.

The thickness of corrosion layer at the concrete surface cracks is regarded <100 μm according to Wong (2010), Zhao and Jin (2006), and Zhao, Karimi et al. (2011), which is much smaller than the critical CL thickness when the CP is constant, approximately 300 μm (Zhao et al., 2013). Therefore, the CP thickness did not reach the maximum value before the concrete surface cracked, i.e., it is somewhere in the sideling line in Figure 2. Therefore, the first half equations of $\overline{T_{CP}}$ and $T_{CL,\,pore}$ when $\overline{T_{CL}} < T_{CL}^{cr}$ in Eqs (3) and (5) will be used in the concrete surface cracking model.

2.3 Nominal ratio between the corrosion products volume and the basic steel volume

If the volume of original steel corroded is defined as V_{steel} and the volume of the total rust generated from the basic steel is V_{rust}, then the ratio between the corrosion products volume and the basic steel volume n can be expressed as follows:

$$n = \frac{V_{rust}}{V_{steel}} \tag{6}$$

where n normally varies from 2 to 6 (Cornell & Schwertmann, 1996; Marcotte & Hansson, 2007).

In the actual process of concrete cracking caused by steel corrosion, some corrosion products form the corrosion layer, and the other products fill the adjacent concrete pores. The total volume of corrosion, V_{rust}, is the sum of the two parts:

$$V_{rust} = V_{rust,\,CP} + V_{rust,\,CL} \tag{7}$$

where $V_{rust,\,CP}$ is the volume of corrosion that forms the CP, and $V_{rust,\,CL}$ is the volume of corrosion that generates the corrosion layer (CL), which actually contributes to the expansive pressure and induces the concrete cracking. Therefore, we define the nominal ratio between the corrosion product volume and the basic steel volume, n_0, as follows:

$$n_0 = \frac{V_{rust,\,CL}}{V_{steel}} \tag{8}$$

The relationship between n_0 and n is expressed as follows:

$$n_0 = \frac{n}{\alpha_n} \tag{9}$$

where α_n is the conversion coefficient, as follows:

$$\alpha_n = \frac{n}{n_0} = \frac{V_{rust}/V_{steel}}{V_{rust,\,CL}/V_{steel}} = \frac{V_{rust,\,CL} + V_{rust,\,CP}}{V_{rust,\,CL}} = 1 + \frac{V_{rust,\,CP}}{V_{rust,\,CL}} \tag{10}$$

The rust volume can be approximately by the rust thickness as

$$\frac{V_{rust,\,CP}}{V_{rust,\,CL}} \approx \frac{T_{rust,\,CP}}{T_{rust,\,CL}} = \frac{T_{CL,\,pore}}{T_{CL}} \tag{11}$$

Combining Eqs (10) and (11), the following relation is obtained:

$$\alpha_n = 1 + \frac{T_{CL,\,pore}}{T_{CL}} \tag{12}$$

Equation (10) shows that a larger α_n results in a larger $V_{rust,\,CP}$, indicating more corrosion in the concrete pores. If $\alpha_n = 1.0$, then the corrosion filling into the concrete pores in the steel/concrete interface is neglected.

According to Eqs (5) and (12), before concrete surface cracking, α_n can be represented as follows:

$$\alpha_n = 1 + \phi \times k_T \tag{13}$$

Equation (13) shows that as ϕ increases, α_n also increases, indicating that concrete with larger porosity can accommodate more corrosion products.

3. CORROSION-INDUCED CONCRETE CRACKING PROCESS ANALYSIS

3.1 Non-cracking stage of corrosion-induced concrete cracking process

Figure 4 shows the schematic diagrams used in the analysis, where C is the thickness of the concrete cover, R is the radius of the steel bar, d is the nominal diameter of the steel bar with free-expansion corrosion products, q is the expansive pressure induced at the steel/concrete interface, d_p is the residual diameter of the steel bar after corrosion, δ_c and δ_r are the radial deformation of the concrete and the corrosion products at concrete/corrosion products interface, respectively.

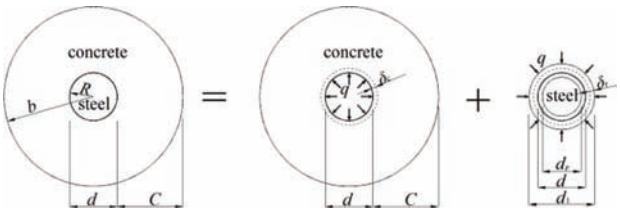

Figure 4. Deformations of rust layer and surrounding concrete under expansive pressure in the non-cracking stage.

According to elastic mechanics, the stresses of a thick-walled cylinder subjected to an internal radial pressure are expressed as follows (Timoshenko & Goodier, 1970):

$$\begin{cases} \sigma_r = \dfrac{qR^2}{b^2 - R^2}\left(1 - \dfrac{b^2}{r^2}\right) \\ \sigma_\theta = \dfrac{qR^2}{b^2 - R^2}\left(1 + \dfrac{b^2}{r^2}\right) \end{cases} \tag{14}$$

where $b = R + C$, σ_r, and σ_θ are the radial and hoop stresses induced by steel corrosion in concrete cover, respectively. The strains are also expressed as (Timoshenko & Goodier, 1970):

$$\begin{cases} \varepsilon_r^e = \dfrac{1+\nu_c}{E_c}\dfrac{qR^2}{b^2 - R^2}\left(1 - 2\nu_c - \dfrac{b^2}{r^2}\right) \\ \varepsilon_\theta^e = \dfrac{1+\nu_c}{E_c}\dfrac{qR^2}{b^2 - R^2}\left(1 - 2\nu_c + \dfrac{b^2}{r^2}\right) \end{cases} \tag{15}$$

where E_c is the elastic modulus of concrete, ν_c is the Poisson's ratio of concrete, $\nu_c = 0.3$ in the study as it tends to get larger at a higher stress level (Guo, 1999), ε_r^e and ε_θ^e are the radial and hoop elastic strains induced by steel corrosion in concrete cover, respectively. As there has been plastic strain in concrete at the cracking moment, the elastic modulus E_c in Eq. (15) should be replaced by the deformation modulus at the maximum tensile stress E_c' in calculating the real strain, which could be expressed as:

$$\begin{cases} \varepsilon_r = \dfrac{1+\nu_c}{E_c'}\dfrac{qR^2}{b^2 - R^2}\left(1 - 2\nu_c - \dfrac{b^2}{r^2}\right) \\ \varepsilon_\theta = \dfrac{1+\nu_c}{E_c'}\dfrac{qR^2}{b^2 - R^2}\left(1 - 2\nu_c + \dfrac{b^2}{r^2}\right) \end{cases} \tag{16}$$

The deformation modulus at the maximum tensile stress $E_c = 0.5E_c'$ (Shu, 2003). Since $\varepsilon_r = \dfrac{\partial u_r}{\partial r}$, the deformation could be expressed as:

$$u_r = \frac{1+\nu_c}{E_c'}\frac{qR^2}{b^2 - R^2}\left(1 - 2\nu_c + \frac{b^2}{R^2}\right)r \tag{17}$$

where ε_r and ε_θ are the radial and hoop strains induced by steel corrosion in concrete cover, respectively, u_r is the radial deformation.

The concrete cylinder is assumed to crack when the hoop tensile strain at the interface between the steel and the concrete has reached the ultimate tensile strain of concrete, i.e., $\varepsilon_\theta\big|_{r=R} = \varepsilon_t = \dfrac{f_t}{E_c'}$, where ε_t is the ultimate tensile strain of concrete, and f_t is the ultimate tensile strength of concrete. According to Eq. (16), at the inner cracking moment, the expansive pressure $q = q^{inner}$ can be expressed as,

$$q^{inner} = \frac{E_c'}{1+\nu_c} \cdot \frac{\varepsilon_t (b^2 - R^2)}{R^2} \cdot \frac{1}{1 - 2\nu_c + b^2/R^2} \tag{18}$$

The deformation compatibility of concrete and corrosion products, according to Zhao and Jin (2006), can be expressed as follows:

$$R + \delta_c = R_1 + \delta_r \tag{19}$$

where R_1 is the nominal radius of the steel bar with free-expansion corrosion products; $R_1 = R\sqrt{(n_0 - 1)\rho + 1}$. The deformation of concrete δ_c and corrosion products δ_r has been put in the results of Zhao and Jin (2006). Since only the corrosion products that generate the corrosion layer (CL), but not all the corrosion products, contributes to the expansive pressure, the ratio between the corrosion product volume and the basic

steel volume n should be replaced by the nominal volume expansion rate n_0, that is:

$$\begin{cases} \delta_c = u_r = \dfrac{1+\nu_c}{E_c'}\dfrac{qR^2}{b^2-R^2}\left(1-2\nu_c+\dfrac{b^2}{R^2}\right)R \\ \delta_r = -\dfrac{n_0(1-\nu_r^2)R\cdot\sqrt{(n_0-1)\rho+1}}{E_r\{[(1+\nu_r)n_0-2]+2/\rho\}}\cdot q \end{cases} \quad (20)$$

where E_r and ν_r are the elastic modulus and Poisson's ratio of the corrosion products, respectively, and ρ is the steel corrosion.

At the inner surface cracking moment, i.e., the moment crack occurs in the steel/concrete surface, $q = q^{\text{inner}}$. According to Eqs (18)–(20), at the inner surface cracking moment, the relationship between the steel corrosion ρ^{inner} and the expansive pressure q^{inner} could be expressed as:

$$q^{\text{inner}} = \frac{\sqrt{(n_0-1)\rho^{\text{inner}}+1}-1}{\dfrac{(1+\nu_c)(R+C)^2+(1-\nu_c)R^2}{E_c'(2R\cdot C+C^2)}+\dfrac{n(1-\nu_r^2)\cdot\sqrt{(n_0-1)\rho^{\text{inner}}+1}}{E_r\{[(1+\nu_r)n_0-2]+2/\rho^{\text{inner}}\}}} \quad (21)$$

With the reference Eq. (18) has put the solution of Eq. (21) as

$$\rho^{\text{inner}} = \frac{x^2-1}{n_0-1} \quad (22)$$

where

$$x = \sqrt[3]{-\frac{N_2}{2}+\sqrt{\left(\frac{N_2}{2}\right)^2+\left(\frac{N_1}{3}\right)^3}}+\sqrt[3]{-\frac{N_2}{2}-\sqrt{\left(\frac{N_2}{2}\right)^2+\left(\frac{N_1}{3}\right)^3}}-\frac{\alpha_2}{3\alpha_1},$$

and $N_1 = \dfrac{\alpha_3}{\alpha_1}-\dfrac{1}{3}\left(\dfrac{\alpha_2}{\alpha_1}\right)^2$, $N_2 = \dfrac{2}{27}\left(\dfrac{\alpha_2}{\alpha_1}\right)^3-\dfrac{1}{3}\left(\dfrac{\alpha_2}{\alpha_1}\right)\left(\dfrac{\alpha_3}{\alpha_1}\right)+\dfrac{\alpha_4}{\alpha_1}$,

$\alpha_1 = M_2 q^{\text{inner}} - M_3$, $\alpha_2 = M_3 + q^{\text{inner}} M_1 M_3$, $\alpha_3 = M_3 - 2(n_0 - 1) - M_2 q^{\text{inner}}$, $\alpha_4 = 2q^{\text{inner}} M_1 (n_0 - 1) + 2(n_0 - 1) - q^{\text{inner}} M_1 M_3 - M_3$, and $M_1 = \dfrac{(1+\nu_c)(R+C)^2+(1-\nu_c)R^2}{E_c'(2RC+C^2)}$,

$M_2 = \dfrac{n_0(1-\nu_r^2)}{E_r}$, $M_3 = (1+\nu_r)n_0 - 2$.

The radial loss of steel at this stage can be expressed as:

$$\delta_{\text{stress}} = (d - d_\rho)/2 \quad (23)$$

where $d_\rho = \sqrt{1-\rho^{\text{inner}}}\cdot d$ is the residual diameter of the steel bar after corrosion.

3.2 Partial cracking stage of corrosion-induced concrete cracking process

After the initiation of cracks at the interface between the steel and the concrete, the cracks in the concrete cylinder propagate along radial direction. Thus, the thick-walled cylinder can be divided into two coaxial cylinders. One is the inner cracked cylinder and the other is the outer intact cylinder, as shown in Figure 5, where R_c is the radius at the interface between the cracked and intact cylinders.

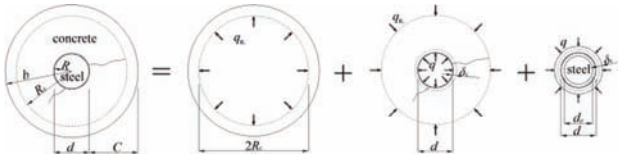

Figure 5. Deformations of rust layer and surrounding concrete under expansive pressure in the partial cracking stage.

The analysis on intact part ($R_c \le r \le b$) is similar with that of non-cracking stage, and the stresses and strains at any point of the intact concrete cylinder could be expressed as follows:

$$\begin{cases} \sigma_r = \dfrac{q_{R_c}R_c^2}{b^2-R_c^2}\left(1-\dfrac{b^2}{r^2}\right) \\ \sigma_\theta = \dfrac{q_{R_c}R_c^2}{b^2-R_c^2}\left(1+\dfrac{b^2}{r^2}\right) \end{cases} \quad (24)$$

$$\begin{cases} \varepsilon_r = \dfrac{1+\nu_c}{E_c'}\dfrac{q_{R_c}R_c^2}{b^2-R_c^2}\left(1-2\nu_c-\dfrac{b^2}{r^2}\right) \\ \varepsilon_\theta = \dfrac{1+\nu_c}{E_c'}\dfrac{q_{R_c}R_c^2}{b^2-R_c^2}\left(1-2\nu_c+\dfrac{b^2}{r^2}\right) \end{cases} \quad (25)$$

where q_{R_c} is the radial pressure at the interface between the intact and cracked cylinder.

For inner cracked concrete cylinder, the damage of concrete cover varies along the radial direction. A damage variable, based on Mohr–Coulomb failure criterion (Mohr, 1900) and Mazar's damage model (Lemaitre, 1990), is adopted here to describe the different damage along the radial direction of the concrete cover.

The governing equation for equilibrium in the axisymmetric case can be expressed as follows (Timoshenko & Goodier, 1970):

$$\frac{\mathrm{d}\sigma_r}{\mathrm{d}r}+\frac{\sigma_r-\sigma_\theta}{r}=0 \quad (26)$$

According to Mohr–Coulomb failure criterion with a damage variable D, the relationship between two stress components can be obtained (Shen & Yang, 2009):

$$\sigma_\theta = \sigma_r\frac{1+(1-D)\sin\varphi}{1-(1-D)\sin\varphi}+\frac{2c\cos\varphi}{1-(1-D)\sin\varphi} \quad (26a)$$

where c and φ are the cohesive strength and internal friction angle of concrete, respectively. The c, φ, and D can be obtained (Li, Ge, Mi, & Zhang, 2004; Shen & Yang, 2009):

$$\begin{cases} c = \dfrac{1}{2}\sqrt{f_t \cdot f_c} \\ \varphi = 90^\circ - \dfrac{360^\circ}{\pi} \cdot \arctan\sqrt{\dfrac{f_t}{f_c}} \end{cases} \tag{26b}$$

$$D = 1 - \frac{\varepsilon_t(1-A_t)}{\varepsilon_\theta} - \frac{A_t}{\exp\left[B_t(\varepsilon_\theta - \varepsilon_t)\right]} \tag{26c}$$

where f_c is the compressive strength of the concrete, and A_t and B_t are coefficients of Mazar's damage model, $0.7 < A_t < 1$, $10^4 < B_t < 10^5$.

Substituting Eq. (26a) into Eq. (26) yields,

$$\sigma_r = e^{-\int_R^r \frac{2(1-D)\sin\phi}{[1+(1-D)\sin\phi]x}\mathrm{d}x} \cdot \left(\int_R^r \frac{2c\cos\phi}{\xi\left[1+(1-D)\sin\phi\right]} \cdot e^{\int_R^\xi \frac{2(1-D)\sin\phi}{[1+(1-D)\sin\phi]x}\mathrm{d}x} \mathrm{d}\xi + C_0 \right) \tag{27}$$

Using the following boundary conditions:

$$\sigma_r = -q \text{ at } r = R \tag{28}$$

$$\begin{cases} D = 0 \\ \sigma_r = -q_{R_c} \text{ at } r = R_c \\ \varepsilon_\theta = \varepsilon_t \end{cases} \tag{29}$$

Substituting Eq. (35) into Eqs (31) and (34) yields,

$$q = q_{R_c}\left(\frac{R_c}{R}\right)^{\frac{2\sin\phi}{1+\sin\phi}} + \frac{c\cos\phi}{\sin\phi}\left[\left(\frac{R_c}{R}\right)^{\frac{2\sin\phi}{1+\sin\phi}} - 1\right] \tag{30}$$

To simplify calculation, the cracked part is divided into N rings of equal thickness, as shown in Figure 6 and the damage variable D within each ring is assumed to be constant.

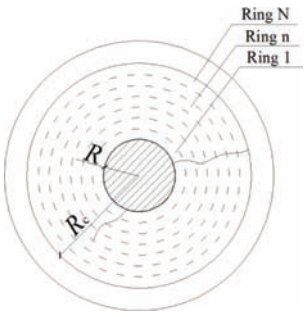

Figure 6. Cracked section partitions (Zhao, Yu et al., 2011).

The radial displacement u_r in the cracked cylinder can be expressed as follows (Li et al., 2004):

$$\frac{\mathrm{d}^2 u_r}{\mathrm{d}r^2} + \frac{1}{r}\frac{\mathrm{d}u_r}{\mathrm{d}r} - k\frac{u_r}{r^2} = 0,\ k = 1 - D \tag{31}$$

$$u_r = C_1 r^{\sqrt{1-D}} + C_2 r^{-\sqrt{1-D}} \tag{32}$$

$$\begin{cases} \varepsilon_r = C_1\sqrt{1-D}\,r^{\sqrt{1-D}-1} - C_2\sqrt{1-D}\,r^{-\sqrt{1-D}-1} \\ \varepsilon_\theta = C_1 r^{\sqrt{1-D}-1} + C_2 r^{-\sqrt{1-D}-1} \end{cases} \tag{33}$$

where C_1 and C_2 are constants.

Assuming that the thickness of each ring is ΔR, so the thickness of the crack part is $N \cdot \Delta R$. For Ring N shown in Figure 6, the constants C_1^N and C_2^N could be calculated based on the Eq. (33) and the corresponding boundary conditions in Eqs (28) and (29). Since the inner surface of Ring N is the outer surface of Ring $N-1$, the constants of Ring $N-1$, i.e., C_1^{N-1} and C_2^{N-1} could be calculated based on the conditions of compatibility of strain. Similarly, the constants and strains from Ring $N-2$ to Ring 1 could be calculated. The deformation of concrete at the steel/concrete interface is equal to u_r^1, that is

$$\delta_c = u_r^1 = C_1^1 R^{\sqrt{1-D^1}} + C_2^1 R^{-\sqrt{1-D^1}} \tag{34}$$

where u_r^1 is the radial displacement of Ring 1 in Figure 6 and D^1 is the damage value of Ring 1. The radial loss of steel at this stage can also be calculated similar with Eqs (18)–(23). When the cracks reach the surface of the concrete, i.e., $R_c = R + C$, the radial loss of steel calculated as the method above is thus the radial loss of steel $\delta_{\text{steel}}^{\text{surface}}$.

The specific partial cracking process is mainly based on the authors' previous study (Zhao, Yu et al., 2011). According to the definition of n_0 in Section 2.3, the corrosion layer thickness at the concrete surface cracking moment, $T_{\text{CL}}^{\text{surface}}$, can be expressed as follows:

$$T_{\text{CL}}^{\text{surface}} = n_0 \cdot \delta_{\text{steel}}^{\text{surface}} - \delta_r \tag{35}$$

4. CONCLUSION

The following conclusions have been drawn from this study:

(1) A T_{CP}–T_{CL} model, describing the relation between the thickness of CP and that of CL, was proposed. The parameter k_T in this model was used to describe the phenomenon that the corrosion filling in the concrete pores and accumulating at the steel/concrete interface occur synchronously.

(2) The nominal ratio between the corrosion product volume and the basic steel volume, n_0, was

introduced to include the corrosion products in the CP layer. α_n, i.e., the ratio between n_0 and n, was defined as a conversion coefficient to indicate the capacity of concrete to accommodate corrosion products.

(3) A corrosion-induced cracking model was proposed. In the model, the phenomena of corrosion layer accumulation and corrosion filling occur simultaneously in concrete.

ACKNOWLEDGMENT

Financial support from the National Natural Science Foundation of China with Grant No. 51278460 is gratefully acknowledged.

REFERENCES

Andrade, C., Alonso, C., & Molina, F. J. (1993). Cover cracking as a function of bar corrosion: Part 1 – Experimental test. *Materials Structures, 26*, 453–464.

Asami, K., & Kikuchi, M. (2003). In-depth distribution of rusts on a plain carbon steel and weathering steels exposed to coastal-industrial atmosphere for 17 years. *Corrosion Science, 45*, 2671–2688.

Bazant, Z. P. (1979). Physical model for steel corrosion in sea structures-applications. *Journal of the Structural Division, 105*, 1137–1153.

Care, S., Nguyen, Q. T., L'Hostis, V., & Berthaud, Y. (2008). Mechanical properties of the rust layer induced by impressed current method in reinforced mortar. *Cement and Concrete Research, 38*, 1079–1091.

Chitty, W. J., Dillmann, P., Hostis, V. L., & Lombard, C. (2005). Long-term corrosion resistance of metallic reinforcements in concrete – A study of corrosion mechanisms based on archaeological artifacts. *Corrosion Science, 47*, 1555–1581.

Cornell, R. M., & Schwertmann, U. (1996). *The iron oxides*. Weinhaim, Germany: VHC Verlagsgesellschaft.

Duffó, G. S., Morris, W., Raspini, I., & Saragovi, C. (2004). A study of steel rebars embedded in concrete during 65 years. *Corrosion Science, 46*, 2143–2157.

Guo, Z. H. (1999). *The strength and deformation of concrete – Experimental basis and constitutive relation*. Beijing, China: Tsinghua University Press. (in Chinese).

Hansen, E. J., & Saouma, V. E. (1999). Numerical simulation of reinforced concrete deterioration: Part II – Steel corrosion and concrete cracking. *ACI Material Journal, 96*, 331–338.

Hartt, W. H. (2012). Service life projection for chloride-exposed concrete reinforced with black and corrosion-resistant bars. *Corrosion, 68*, 754–761.

Jaffer, S. J., & Hansson, C. M. (2009). Chloride-induced corrosion products of steel in cracked-concrete subjected to different loading conditions. *Cement Concrete Research, 39*, 116–125.

Kim, K. H., Jang, S. Y., Jang, B. S., & Oh, B. H. (2010). Modeling mechanical behavior of reinforced concrete due to corrosion of steel bar. *ACI Structural Journal, 107*, 106–113.

Lemaitre, J. (1990). *A course on damage mechanics* (2nd ed.). Berlin, Germany: Springer, p. 1990.

Li, C. Q., Melchers, R. E., & Zheng, J. J. (2006). Analytical model for corrosion-induced crack width in reinforced concrete structures. *ACI Structural Journal, 103*, 479–487.

Li, Y. A., Ge, X. R., Mi, G. R., & Zhang, H. C. (2004). Failure criteria of rock-soil-concrete and estimation of their strength parameters. *Chinese Journal of Rock Mechanics and Engineering, 23*, 770–776. (in Chinese).

Liu, Y. P., & Weyers, R. E. (1998). Modeling the time-to-corrosion cracking in chloride contaminated reinforced concrete structures. *ACI Structural Journal, 95*, 675–681.

Lu, C. H., Jin, W. L., & Liu, R. G. (2011). Reinforcement corrosion-induced cover cracking and its time prediction for reinforced concrete structures. *Corrosion Science, 53*, 1337–1347.

Malumbela, G., Alexander, M., & Moyo, P. (2011). Model for cover cracking of RC beams due to partial surface steel corrosion. *Construction and Building Materials, 25*, 987–991.

Marcotte, T. D., & Hansson, C. M. (2007). Corrosion products that form on steel within cement paste. *Material Structures, 40*, 325–340.

Michel, A., Pease, B. J., Geiker, M. R., Stang, H., & Olesen, J. F. (2011). Monitoring reinforcement corrosion and corrosion-induced cracking using nondestructive X-ray attenuation measurements. *Cement and Concrete Research, 41*, 1085–1094.

Mohr, O. (1900). Welche Umstände bedingen die Elastizitätsgrenze und den Bruch eines Materials. *Zeitschrift des Vereins Deutscher Ingenieure, 46*, 1572–1577.

Molina, F. J., Alonso, C., & Andrade, C. (1993). Cover cracking as a function of rebar corrosion: Part 2 – Numerical model. *Material Structures, 26*, 532–548.

Ohtsu, M., & Yosimura, S. (1997). Analysis of crack propagation and crack initiation due to corrosion of reinforcement. *Construction and Building Materials*, *11*, 437–442.

Shen, X. P., & Yang, L. (2009). *Concrete damage theory and experiments*. Beijing, China: Science Press. (in Chinese).

Shu, S. L. (2003). *Reinforced concrete structures* (2nd ed.). Hangzhou, China: Zhejiang University Press. (in Chinese).

Timoshenko, S. P., & Goodier, J. N. (1970). *Theory of elasticity* (3rd ed.). New York, NY: McGraw-Hill Book Company.

Williamson, S. J., & Clark, L. A. (2000). Pressure required to cause cover cracking of concrete due to reinforcement corrosion. *Magazine of Concrete Research, 52*, 455–467.

Wong, H. S., Zhao, Y. X., Karimi, A. R., Buenfeld, N. R., & Jin, W. L. (2010). On the penetration of corrosion products from reinforcing steel into concrete due to chloride-induced corrosion. *Corrosion Science, 52*, 2469–2480.

Zhao, Y. X., Ding, H. J., & Jin, W. L. (2014). Corrosion layer at the steel/concrete interface. *Corrosion Science, 87*, 199–210.

Zhao, Y. X., & Jin, W. L. (2006). Modeling the amount of steel corrosion at the cracking of concrete cover. *Advances in Structural Engineering, 9*, 687–696.

Zhao, Y. X., Karimi, A. R., Wong, H. S., Hu, B. Y., Buenfeld, N. R., & Jin, W. L. (2011). Comparison of uniform and non-uniform corrosion induced damage in reinforced concrete based on a Gaussian description of the corrosion layer. *Corrosion Science, 53*, 2803–2814.

Zhao, Y. X., Wu, Y. Y., & Jin, W. L. (2013). Distribution of millscale on corroded steel bars and penetration of steel corrosion products in concrete. *Corrosion Science, 66*, 160–168.

Zhao, Y. X., Yu, J., Hu, B. Y., & Jin, W. L. (2012). Crack shape and rust distribution in corrosion induced cracking concrete. *Corrosion Science, 55*, 385–393.

Zhao, Y. X., Yu, J., & Jin, W. L. (2011). Damage analysis and cracking model of reinforced concrete structures with rebar corrosion. *Corrosion Science, 53*, 3388–3397.

Zhao, Y. X., Yu, J., Wu, Y. Y., & Jin, W. L. (2012). Critical thickness of rust layer at inner and out surface cracking of concrete cover in reinforced concrete structures. *Corrosion Science, 59*, 316–323.